BIOCHEMISTRY
including biophysical chemistry & molecular biology
Article

*Biochemistry* **2010,** *49,* 8445–8454 8445
DOI: 10.1021/bi100984j

# DNA Binding Induces Dimerization of *Saccharomyces cerevisiae* Pif1

Sergio Barranco-Medina[‡] and Roberto Galletto*[,‡]

*Department of Biochemistry and Molecular Biophysics, Washington University School of Medicine, Saint Louis, Missouri 63110.*
*[‡]Both authors contributed equally to this work.*

*Received June 17, 2010; Revised Manuscript Received August 18, 2010*

ABSTRACT: In *Saccharomyces cerevisiae*, Pif1 is involved in a wide range of DNA transactions. It operates both in mitochondria and in the nucleus, where it has telomeric and non-telomeric functions. All of the activities of Pif1 rely on its ability to bind to DNA. We have determined the mode of Pif1 binding to different DNA substrates. While Pif1 is a monomer in solution, we show that binding of ssDNA to Pif1 induces protein dimerization. DNA-induced dimerization of Pif1 is also observed on tailed- and forked-dsDNA substrates, suggesting that on the latter formation of a Pif1 dimer prevents binding of additional Pif1 molecules. A dimer of Pif1 also forms on ssDNA of random composition and in the presence of saturating concentrations of nonhydrolyzable ATP analogues. The observation that a Pif1 dimer is formed on unwinding substrates in the presence of ATP analogues suggests that a dimeric form of the enzyme might constitute the pre-initiation complex leading to its unwinding activity.

In budding yeast *Saccharomyces cerevisiae*, a complex interplay of helicases in telomere regulation is emerging. Multiple helicases have been reported to have either direct or indirect roles in telomere function: Pif1, Rrm3, Dna2, Sgs1, and Srs2 (*1*−*6*). Of these helicases, Pif1 (petite integration frequency 1) is the only helicase for which a direct effect on the telomerase, the reverse transcriptase responsible for extension of the 3′-end of chromosome ends, has been reported (*2*, *7*). Pif1 is produced in two variants from different translation start sites (*3*, *8*, *9*). The full-length Pif1 helicase is targeted to mitochondria, while a shorter variant, missing the first 40 N-terminal amino acids, is localized in the nucleus (*3*, *8*, *9*). The nuclear form of Pif1 has both telomeric and non-telomeric functions. At telomeres, Pif1 acts as a negative regulator of telomere metabolism, inhibiting telomere elongation and *de novo* telomere addition (*2*, *7*, *9*). The mitochondrial form of Pif1 participates in mtDNA repair and recombination (*8*, *10*, *11*).

*PIF1* has been shown to participate in mtDNA repair after UV or ethidium bromide damage and in mtDNA maintenance at high temperatures (*8*, *12*). More recently, a direct role of *PIF1* in preventing mtDNA instability due to oxidative stress has been described (*10*). Partial purification of the mitochondrial Pif1 protein showed for the first time that the protein is a 5′ to 3′ helicase, whose ATPase activity is highly stimulated by ssDNA[1] (*8*, *12*).

The nuclear version of Pif1 has been implicated in a wide array of pathways. Pif1 functions in replication fork progression at rDNA sites (*13*). Also, the helicase activity of Pif1 is involved in Okazaki fragment processing in conjunction with the activity of Dna2 helicase/nuclease (*6*). Notably, genetic screening for the loss of expression of genes positioned at subtelomeric regions identified a mutation in *PIF1* (*9*). This mutation in *PIF1* affects the length and heterogeneity of telomeres and causes a large increase in the *de novo* addition of new telomeres at the end of broken chromosomes. Moreover, Pif1 helicase participates in the suppression of gross chromosomal rearrangements via suppression of the *de novo* telomere addition pathway (*14*, *15*). The Zakian laboratory showed that the suppression activity of Pif1 on *de novo* telomere addition and on telomere lengthening occurs via direct inhibitory effects of Pif1 on the activity of the telomerase (*7*). In a more recent study, the same laboratory provided evidence that Pif1 directly affects the telomerase and causes it to dissociate from the telomeric end (*2*). Biochemical studies on the unwinding activity of Pif1 strongly suggest that RNA−DNA heteroduplexes are unwound with higher efficiency than dsDNA (*16*). Thus, it has been suggested that the function of Pif1 in the displacement of the telomerase is simply to unwind the RNA−DNA heteroduplex formed by the telomeric TLC1 RNA of the telomerase and the ssDNA at telomeres (*2*, *3*, *16*). Finally, studies of the substrate requirement for its helicase activity indicate that Pif1 preferentially unwinds dsDNA substrates with a 5′-ssDNA overhang (*16*). However, the presence of a 3′-ssDNA tail in combination with a 5′-overhang (fork substrates) increases the efficiency of the unwinding reaction (*16*).

Although it is evident that all of the activities of Pif1 require binding to DNA, the mode of Pif1−DNA interaction is not known. While it has been shown that Pif1 binds to ssDNA with relatively high affinity (*2*, *16*), the stoichiometry of interaction remains unexplored. In this study, we applied quantitative approaches to determine the mode of binding of Pif1 to DNA. Our data show a more complex mode of Pif1−DNA interaction than previously assumed. Binding of Pif1 to ssDNA is characterized by a DNA-induced dimerization of the protein. The same mode of interaction is maintained on unwinding substrates and on sequences of random composition, and it is independent of the nucleotide-bound state of Pif1. Possible implications of the observed Pif1 dimerization on DNA for its function are discussed.

*To whom correspondence should be addressed: 252 McDonnell Science Building, Washington University, School of Medicine, Department of Biochemistry and Molecular Biophysics, 660 S. Euclid Ave., MS8231, Saint Louis, MO 63110. Phone: (314) 362-4368. Fax: (314) 362-7183. E-mail: galletto@biochem.wustl.edu.

[1]Abbreviations: ssDNA, single-stranded DNA; dsDNA, double-stranded DNA; AMP-PNP, adenosine 5′-(β,γ-imido)triphosphate; ATPγS, adenosine 5′-[γ-thio]triphosphate; Tris, tris(hydroxymethyl)aminomethane; EDTA, ethylenediaminetetraacetic acid; DTT, dithiothreitol.


Published on Web 08/26/2010

## MATERIALS AND METHODS

*Reagents and Buffers*. All chemicals were reagent grade. All solutions were made with distilled and deionized 18 MΩ (Milli-Q) water (Millipore Corp., Bedford, MA). The oligonucleotides were purchased from Integrated DNA Technology (IDT, Coralville, IA) and HPLC purified. Oligonucleotide concentrations were determined in 10 mM Tris-HCl (pH 8.3) and 0.1 mM EDTA using extinction coefficients ($\varepsilon_{260}$) of 8100 $M^{-1}$ $cm^{-1}$ for dT and 20960 $M^{-1}$ $cm^{-1}$ for fluorescein (*17*). For oligonucleotides with a mixed sequence composition, the extinction coefficient is calculated with the nearest-neighbor method (*18*−*20*). The sequences for generating the dsDNA substrates contain a constant duplex region of 15 bp and variable lengths of 5′- or 3′-ssDNA. Strand 1 is 5′-$dT_n$CCGGGGCCGCGCCGC and strand 2 3′-$dT_m$GGCCCCGGCGCGGCG, where *n*, *m*, and the position of the fluorescein label are indicated in the figures. We prepared all the dsDNA substrates by annealing a 1.1:1 ratio of unlabeled to labeled strand in 10 mM Tris-HCl (pH 8.3), 100 mM NaCl, and 5 mM $MgCl_2$ for 5 min at 97 °C and then slowly cooling the samples to room temperature. The concentration of nonhydrolyzable ATP analogues AMP-PNP and ATPγS (Sigma-Aldrich, St. Louis, MO) was determined using an $\varepsilon_{259}$ of 15400 $M^{-1}$ $cm^{-1}$.

*Cloning, Overexpression, and Purification of Pif1 Helicase*. The initial pET28b expression plasmid for Pif1 was a kind gift of V. Zakian (Princeton University, Princeton, NJ). *PIF1* was recloned into the pET30a vector (Recombinant DNA Laboratory, University of Texas Medical Branch, Galveston, TX) for expression of the full-length, untagged protein. Freshly transformed expression strains Rosetta2(DE3)pLysS (EMD Chemicals, Novagene, Gibbstown, NJ) were used to inoculate a 16 L fermenter culture (Mobile Pilot Plant Fermenter, New Brunswick Scientific). The cells were allowed to grow at 37 °C until the OD reached 0.6−0.7, quickly chilled and induced with 1 mM IPTG at ~30 °C, and grown overnight at 18 °C. Pif1 carrying the K264A mutation in the Walker A motif of the ATPase site ($Pif1^{K264A}$) was generated by PCR mutagenesis (QuickChange Lightening, Stratagene) using the original pET28b vector and expressed as an N-terminal $His_6$-tagged protein.

We established a purification protocol that yields a final Pif1 protein that is at least 97% pure as judged by Coomassie Blue staining (Supporting Information). The concentration of Pif1 was determined spectrophotometrically with a Cary 100 instrument (Varian Inc., Palo Alto, CA) using an extinction coefficient $\varepsilon_{280}$ of 55000 $M^{-1}$ $cm^{-1}$, which is an average of the one calculated from the amino acid composition and the one experimentally determined under denaturing conditions (*21*, *22*). Pif1 carrying the K264A mutation in the Walker A motif of the ATPase site ($Pif1^{K264A}$) was overexpressed and purified with a protocol similar to that used for the wild type (Supporting Information).

*Fluorescence Titrations*. All fluorescence experiments were performed with a L-format PC1 spectrofluorimeter (ISS, Champaign, IL) equipped with Glenn-Thompson polarizers. The change in anisotropy of fluorescein-labeled DNA was determined using excitation and emission wavelengths of 490 and 530 nm, respectively, with slit widths of 1 mm. Each anisotropy value is determined from an average of 10 readings. The standard deviation of the reported values of anisotropy is less than 4%, as determined from multiple titrations over multiple Pif1 preparations.

*Analytical Ultracentrifugation*. All experiments were conducted with an Optima XL-A analytical ultracentrifuge and an An60Ti rotor (Beckman Coulter, Brea, CA). Sedimentation velocity experiments were performed with an Epon charcoal-filled double-sector centerpiece at 50000−55000 rpm. For experiments with Pif1 alone, the samples were scanned at 280 nm every 8 min at a spacing of 0.03 cm. For experiments with Pif1 in the presence of labeled DNA, the samples were scanned at 495 nm (fluorescein), where protein absorption does not contribute to the observed signal. Sedimentation velocity profiles were processed and analyzed with SedFit/SedPhat (P. Schuck, National Institute of Biomedical Imaging and Bioengineering, National Institutes of Health, Bethesda, MD) (*23*−*26*) and the apparent sedimentation coefficient corrected for temperature and buffer composition [SEDNTERP, by D. Hayes (Magdalen College, Warner, NH), T. Laue (University of New Hampshire, Durham, NH), and J. Philo (Alliance Protein Laboratories, Camarillo, CA)].

Sedimentation equilibrium experiments were performed with an Epon charcoal-filled six-sector centerpiece at 12000−22000 rpm. For experiments with Pif1 alone, the samples were scanned at 280 nm every 2 h at a spacing of 0.001 cm and an average of three scans. Achievement of equilibrium (~24 h) was determined from overlap of scans at 4 h separation. For experiments with Pif1 in the presence of labeled DNA, the samples were scanned at 495 nm (fluorescein). Sedimentation equilibrium profiles were processed and analyzed with SedFit/SedPhat (P. Schuck) (*23*−*26*) and the apparent molecular weights determined using the partial specific volume calculated from amino acid composition (0.738 mL/g at 25 °C) and the buffer density corrected for temperature and composition (SEDNTERP). The partial specific volume of Pif1 in complex with DNA was calculated from (*27*)

$$\upsilon_{PD} = \frac{nM_P\upsilon_P + M_D\upsilon_D}{nM_P + M_D} \quad (1)$$

where *n* is the number of Pif1 molecules in the complex, $M_P$ and $M_D$ are the molecular weights of Pif1 and the DNA, respectively, $\upsilon_P$ is the partial specific volume of Pif1 (see above), and $\upsilon_D$ is the partial specific volume of the labeled DNA (0.54−0.59 mL/g) (*28*).

## RESULTS

*Pif1 Is a Monomer in Solution*. Analytical sedimentation velocity analysis shows that Pif1 behaves in solution as a single, homogeneous species. A representative set of sedimentation velocity profiles of 8 μM Pif1 in buffer N100M-10 °C [50 mM Tris-HCl (pH 8.3) at 10 °C, 100 mM NaCl, 5 mM $MgCl_2$, 0.5 mM DTT, and 20% (v/v) glycerol] is shown in Figure 1a. The solid lines are the direct fits of the data to a continuous $c(s)$ distribution of Lamm equation solutions (SedFit) (*23*−*26*). The $c(s)$ distribution as a function of $s_{20,w}$ calculated from the analysis of the velocity profiles using SedFit is shown in Figure 1b. In the range of 2−8 S a single, symmetrical peak is observed in the $c(s)$ distribution, indicating that Pif1 sediments as a single species with a sedimentation coefficient ($s_{20,w}$) of 4.38 ± 0.15 S.

The results of equilibrium analytical ultracentrifugation experiments under different solution conditions are shown in Figure 2. The inclusion of glycerol in the buffer is required to increase protein solubility and achieve equilibrium. The solid lines are the analyses of the equilibrium sedimentation profiles assuming a single sedimenting species (SedPhat, P. Schuck) (*23*−*26*). Under these conditions, more complex mechanisms or the inclusion in the analysis of additional sedimenting species does not improve the quality of the fit. Under all the experimental conditions tested (NaCl concentration, $MgCl_2$ concentration, temperature, and pH), Pif1 has an average $M_W$ of 91 ± 4 kDa,

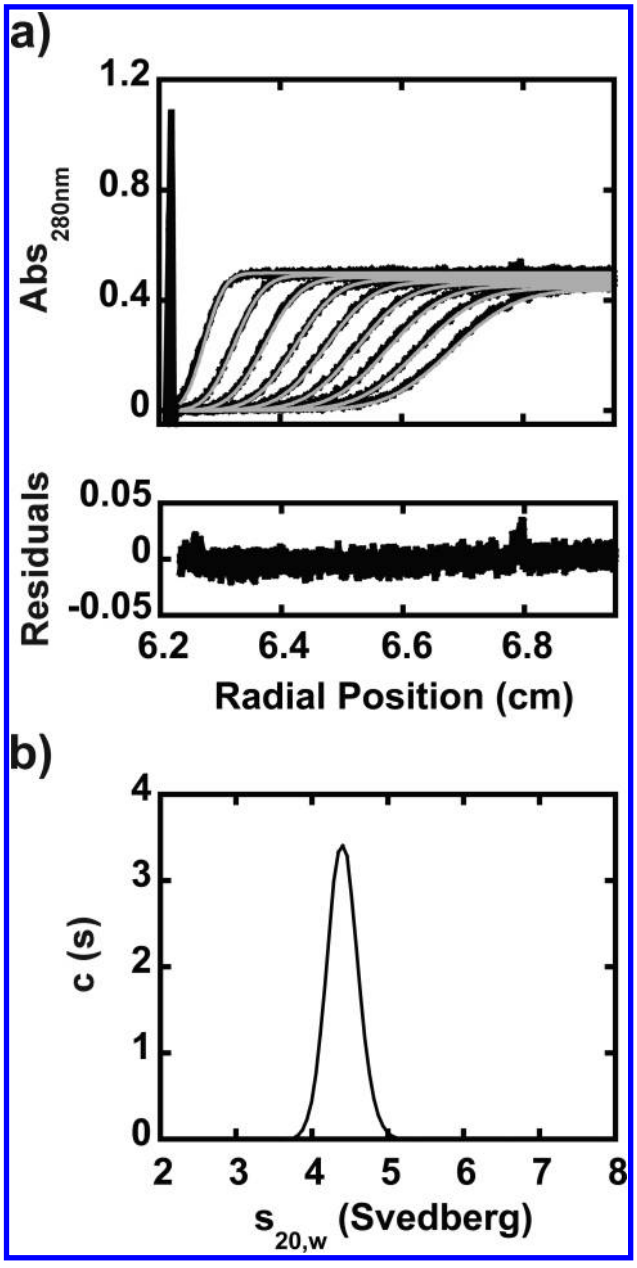


FIGURE 1: Pif1 in solution sediments as a single, homogeneous species. (a) Representative analytical sedimentation velocity profiles recorded at 280 nm and 55000 rpm for 8 $\mu$M Pif1 in buffer N100M-10 °C. The solid lines are the fits of the data to a continuous $c(s)$ distribution of Lamm equation solutions (SedFit). (b) Continuous $c(s)$ distribution as a function of $s_{20,w}$ calculated from the data in panel a.

consistent with the value of 93 kDa calculated from its amino acid composition. Therefore, Pif1 exists as a monomer in solution even at concentrations that are 2−8-fold higher than the highest Pif1 concentration reached in DNA binding studies (see below).

*Pif1 Binds to ssDNA with a 2:1 Stoichiometry*. Interaction of Pif1 with ssDNA is not accompanied by sufficient and reliable changes in the intrinsic fluorescence of the protein. However, binding of Pif1 to homo-oligodeoxynucleotides labeled with fluorescein leads to a large change in the rotational diffusion properties (anisotropy) of the modified oligonucleotide. Furthermore, at saturating Pif1 concentrations, there is a negligible change in the fluorescent quantum yield of the fluorescein-labeled DNA (data not shown). The small change in the quantum yield of the fluorophore will not make a significant contribution to the "distortion" of fluorescence anisotropy induced by differences in quantum yield between the free and bound state of the fluorescent ssDNA (*29*, *30*).

We studied the interaction of Pif1 with ssDNA of different lengths. Even for the shortest length examined (e.g., five nucleotides, data not shown), the interaction cannot be explained with a simple 1:1 binding model. Titrations were performed under tight binding conditions (i.e., stoichiometric titrations), monitoring the change in fluorescence anisotropy as a function of Pif1 concentration of 5′-fluorescein-labeled $dT_n$ (FL-$dT_n$ where $n$ = 6, 8, 14, and 24) in buffer TN100M-10 °C (Figure 3a). The data clearly show that more than one Pif1 molecule binds to the ssDNA under these conditions. For lengths ranging from 6 to 14 nucleotides, the data are consistent with two Pif1 molecules binding to the ssDNA at saturation. Because of the potential multiple, overlapping binding sites, it would be easy to envision that at saturation two Pif1 molecules could bind next to each other on FL-$dT_{14}$, suggesting that the occluded site-size of Pif1 is ∼6−7 nucleotides (Figure 4a, i). If this were the case, a single Pif1 molecule should bind to FL-$dT_6$. However, this is not what we observe. Even on this short ssDNA, at saturation two Pif1 molecules bind to the substrate. It should be noted that if two Pif1 molecules were to bind to FL-$dT_6$ next to each other then the occluded site-size would be ∼2−3 nucleotides, which appears to be physically unreasonable. Moreover, we have been able to exclude experimentally this possibility (see below).

*The Location of the Label Does Not Affect the Mode of Binding of Pif1 to ssDNA*. To assess whether the presence of the label at the 5′-end of the ssDNA has an effect on the observed mode of binding (i.e., stoichiometry), we performed experiments with 3′-end fluorescein-labeled ssDNA. Titration under stoichiometric conditions, monitoring the change in fluorescence anisotropy as a function of Pif1 concentration of 3′-fluorescein-labeled $dT_8$ ($dT_8$-FL) in buffer TN100M-10 °C, is shown in Figure 3b. For comparison, the titration of 5′-fluorescein-labeled $dT_8$ (FL-$dT_8$) under the same conditions is shown as well. It is evident from the data that, independent of the location of the fluorescein label, two Pif1 molecules bind to dT8 at saturation, although the label and its position have an effect on the energetics of the interaction (R. Galletto and S. Barranco-Medina, manuscript in preparation).

*Pif1 Does Not Bind to the End of the ssDNA*. One simple model for explaining the 2:1 stoichiometry observed in Figure 3 would be the binding of Pif1 specifically to the ends of the ssDNA (Figure 4a, ii and iii). In this case, the observed binding constant for ssDNA should be length-independent; however, we do not observe this behavior (R.G. and S.B.-M., in preparation). Alternatively, Pif1 could bind with an extremely small occluded site-size on ssDNA (e.g., 2−3 nucleotides).

If Pif1 does not bind to blunt-end dsDNA, these two possibilities (binding to a free end or an extremely small site-size) can be examined by designing dsDNA substrates with short ssDNA tails. The change in fluorescence anisotropy of dsDNA substrates (15 bp long) with 5′-fluorescein-labeled ssDNA tails of different lengths (FL-$dT_n$-ds15 where $n$ = 0, 2, 3, 4, and 5) as a function of Pif1 concentration in buffer N100M-10 °C is shown in Figure 4b. As a reference, the change in fluorescence anisotropy of ssDNA FL-$dT_5$ under the same buffer conditions is included as well. Binding of Pif1 to a dsDNA with a 5-nucleotide 5′-ssDNA tail is readily detected. Albeit with weaker affinity, Pif1 is able to interact with a dsDNA with a 4-nucleotide ssDNA, while binding of Pif1 to substrates with 5′-ssDNA shorter than 3 nucleotides is

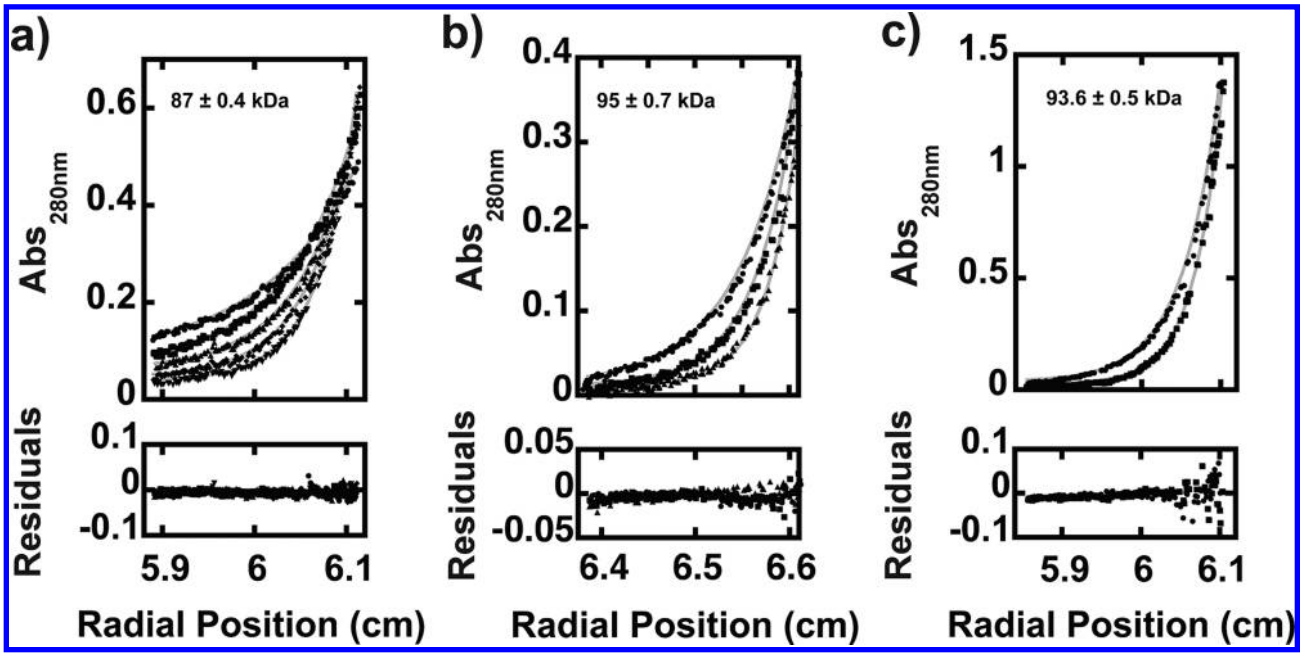


FIGURE 2: Pif1 is monomeric under different solution conditions. Sedimentation equilibrium profiles of Pif1 collected under different experimental conditions. The solid gray lines are the global analyses of each set of data with a single species model (SedPhat), and the obtained $M_w$ values are given. (a) Sedimentation equilibrium profiles of 3.8 $\mu$M Pif1 in buffer H [20 mM Hepes (pH 7.5), 150 mM NaCl, 5 mM $MgCl_2$, 0.5 mM DTT, and 20% (v/v) glycerol] collected at 22 °C, 280 nm, and five different rotor speeds (14000, 16000, 18000, 20000, and 22000 rpm). (b) Sedimentation equilibrium profiles of 2.6 $\mu$M Pif1 in buffer N150E [50 mM Tris-HCl (pH 8.3) at 22 °C, 150 mM NaCl, 0.1 mM EDTA, 0.5 mM DTT, and 20% (v/v) glycerol] collected at 280 nm and three different rotor speeds (16000, 19000, and 22000 rpm). (c) Sedimentation equilibrium profiles of 10 $\mu$M Pif1 in buffer N100M-10 °C (see text) collected at 280 nm and two different rotor speeds (19000 and 22000 rpm).

not detected. These data strongly suggest that in the concentration range examined, Pif1 does not bind to a free end of the ssDNA and that the site-size is not ~2−3 nucleotides (see above). Interestingly, Pif1 binds the dsDNA with a 5-nucleotide 5′-ssDNA tail (FL-$dT_5$-ds15) with an apparent affinity higher than that of a ssDNA of the same length (FL-$dT_5$), suggesting that the presence of the duplex region contributes to the overall affinity of the formed complex (see below).

*Binding of Pif1 to ssDNA Induces Dimerization of the Protein*. Titrations under stoichiometric conditions clearly indicate that Pif1 binding to ssDNA cannot be described by a simple 1:1 interaction. Of the possible models that would account for the observed stoichiometry of two Pif1 molecules bound to a short ssDNA, we can exclude models i−iii in Figure 4a. Next, we tested whether a model in which DNA induces dimerization of Pif1 (Figure 4a, iv) can account for the observed stoichiometry.

The change in fluorescence anisotropy of 25 and 120 nM FL-$dT_7$ as a function of an increasing concentration of Pif1 in buffer N100M-10 °C is shown in Figure 4c. The dotted line is the best fit of the titration at 25 nM FL-$dT_7$ with a simple 1:1 binding model (Supporting Information, eq S7), clearly indicating that it does not represent the data. In addition, the dashed line is the expected behavior of the change in anisotropy for the higher concentration of FL-$dT_7$ (120 nM) and the same parameters determined for a 1:1 binding model. It is evident that this simple binding model does not capture the DNA concentration dependence of the interaction. The solid lines are the analyses of the data with a DNA-induced binding model (Figure 4a, iv) (*31*). The model is described by the following reactions

$$P + D \overset{K}{\leftrightarrow} PD \qquad \text{(Scheme 1)}$$

$$PD + P \overset{L}{\leftrightarrow} P_2D$$

and equations

$$Z = 1 + K[P] + KL[P]^2 \tag{2}$$

$$v = \frac{K[P] + 2KL[P]^2}{Z} \tag{3}$$

$$[P]_T = [P] + v[D]_T \tag{4}$$

where $K$ and $L$ are the DNA binding and the dimerization constants, respectively.

For a system where the change in fluorescence anisotropy is not accompanied by changes in the quantum yield of the fluorophore (see above), the observed anisotropy as a function of the different species in solution is described by (Supporting Information)

$$r_{obs} = \frac{1}{Z} r_D + \frac{K[P]}{Z} r_{PD} + \frac{KL[P]^2}{Z} r_{P_2D} \tag{5}$$

where $r_D$, $r_{PD}$, and $r_{P_2D}$ are the anisotropy values of the free DNA and the DNA in complex with one and two Pif1 molecules, respectively. The anisotropy value of the free DNA is determined before addition of Pif1, and the anisotropy values of the DNA with one and two Pif1 molecules bound are determined from stoichiometric titrations (Figure 3). An independent approach to determining the value of the anisotropy of the singly ligated species is the analysis of the titrations performed at two different concentrations with the general method developed by Bujalowski and Lohman (*32*, *33*) (data not shown). In eq 5, only two parameters, $K$ and $L$, need to be fitted (Micromath, Scientist, St. Louis, MO).

The titrations performed at the two different concentrations of FL-$dT_7$ can be described well by the model in Scheme 1 with an identical set of parameters [Figure 4c; $r_D = 0.09 \pm 0.004$, $r_{PD} = 0.19 \pm 0.005$, $r_{P_2D} = 0.297 \pm 0.03$, $K = (2 \pm 0.5) \times 10^7\ M^{-1}$, and

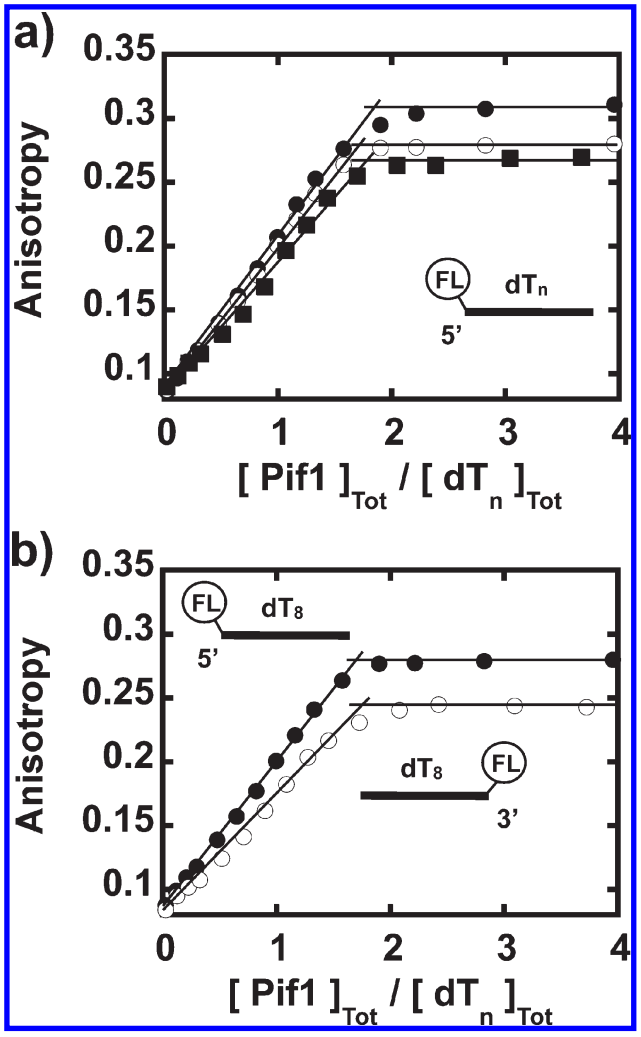


FIGURE 3: At saturation, two Pif1 molecules bind to ssDNA. (a) Change in the fluorescence anisotropy of 5′-FL-labeled $dT_n$ (FL-$dT_n$) at 320 nM with $n$ values of 6 (●), 8 (○), and 14 (■) in buffer N100M-10 °C as a function of the ratio of the total concentrations of Pif1 and DNA. The titrations were performed under conditions of tight binding (stoichiometric). (b) Stoichiometric titrations in buffer N100M-10 °C of 3′-FL-labeled $dT_8$ ($dT_8$-FL) at 320 nM (○) and FL-$dT_8$ (●) at the same concentration. The solid lines in panels a and b are meant for visual help.

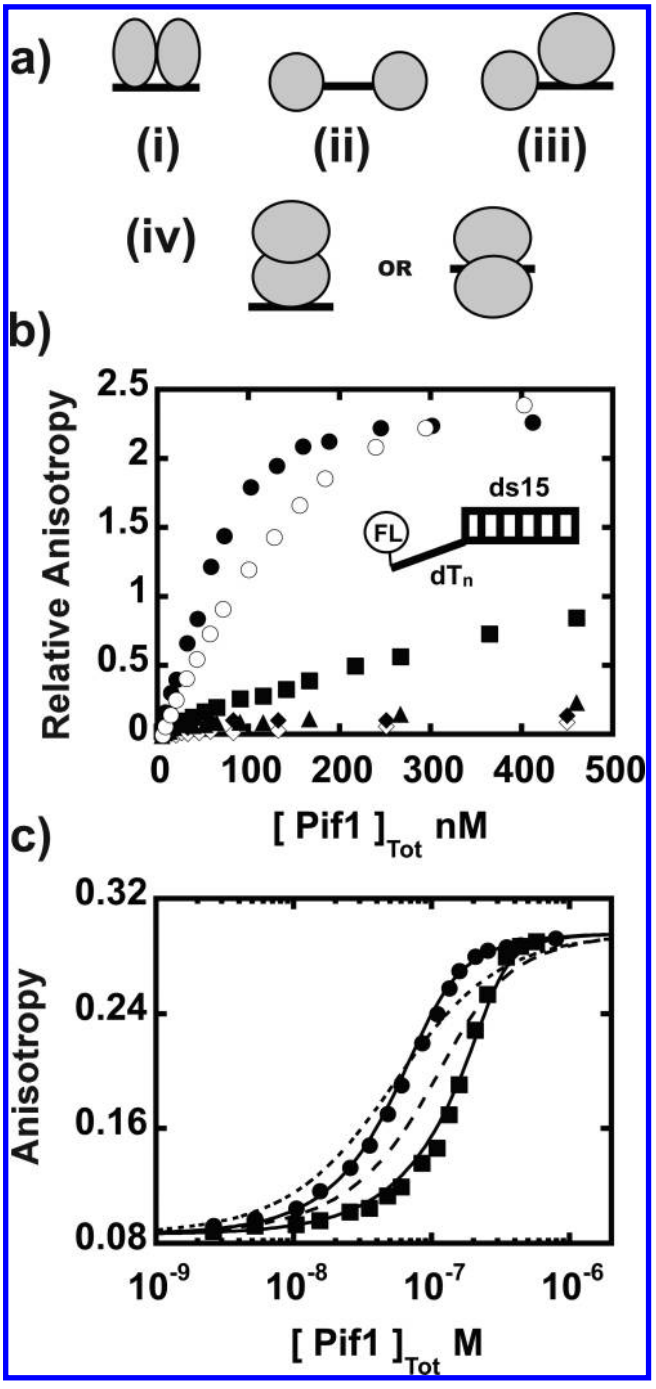


FIGURE 4: Pif1 dimerizes on ssDNA. (a) Four possible models for Pif1 binding to ssDNA that can explain the observed 2:1 stoichiometry. (b) Titrations of the indicated substrates (5′FL-$dT_n$-ds15) at 25 nM with $n$ values of 5 (●), 4 (■), 3 (▲), 2 (◆), and 0 (◇). Also, the titration of 25nM FL-$dT_5$ (○) under the same solution conditions is shown as a reference. (c) Titrations of 25 (●) and 120 nM FL-$dT_7$ (■) with Pif1 in buffer N100M-10 °C. The dotted line is the best fit of the titration at 25 nM Fl-$dT_7$ to a 1:1 model with the following: $r_D$ = 0.09, $r_{PD}$ = 0.297, and $K = 2.5 \times 10^7\ M^{-1}$ (Supporting Information). The dashed line is the expected behavior for the higher concentration of FL-$dT_7$ with the same parameters as for the dotted line. Solid lines are the fits of the titrations at both FL-$dT_7$ concentrations with the same set of parameters [$r_D = 0.09 \pm 0.004$, $r_{PD} = 0.19 \pm 0.005$, $r_{P_2D} = 0.297 \pm 0.03$, $K = (2 \pm 0.5) \times 10^7\ M^{-1}$, and $L = (5 \pm 1) \times 10^7\ M^{-1}$] according to the piggyback model in panel a (iv) (see the text).

$L = (5 \pm 1) \times 10^7\ M^{-1}$]. Thus, the data strongly suggest that the simplest model that can account for the observed behavior of Pif1 interacting with ssDNA is a piggyback model, where binding of Pif1 to ssDNA induces dimerization of the protein (*31*). We would like to point out that the model in Scheme 1 does not allow discrimination between different geometries of the complex (Figure 4, iv). The orientation of the two Pif1 monomers relative to the DNA is currently unknown.

*The Presence of dsDNA Does Not Affect the Mode of Binding*. The data in Figure 4b clearly show that Pif1 does not bind to a blunt end dsDNA substrate and that binding requires a ssDNA tail of at least four nucleotides. Next, we examined whether the presence of a ssDNA−dsDNA junction affects the DNA-induced dimerization of Pif1.

Titrations under stoichiometric conditions of dsDNA substrates with 5′-fluorescein-labeled ssDNA tails of different lengths (FL-$dT_n$-ds15) in buffer N100M-10 °C are shown in Figure 5a. Two Pif1 molecules bind at saturation even for substrates with a 5′-ssDNA tail of only five nucleotides. Increasing the ssDNA tail to twice the length does not change the observed stoichiometry. Therefore, the presence of a ssDNA−dsDNA junction does not affect the mode of binding of Pif1.

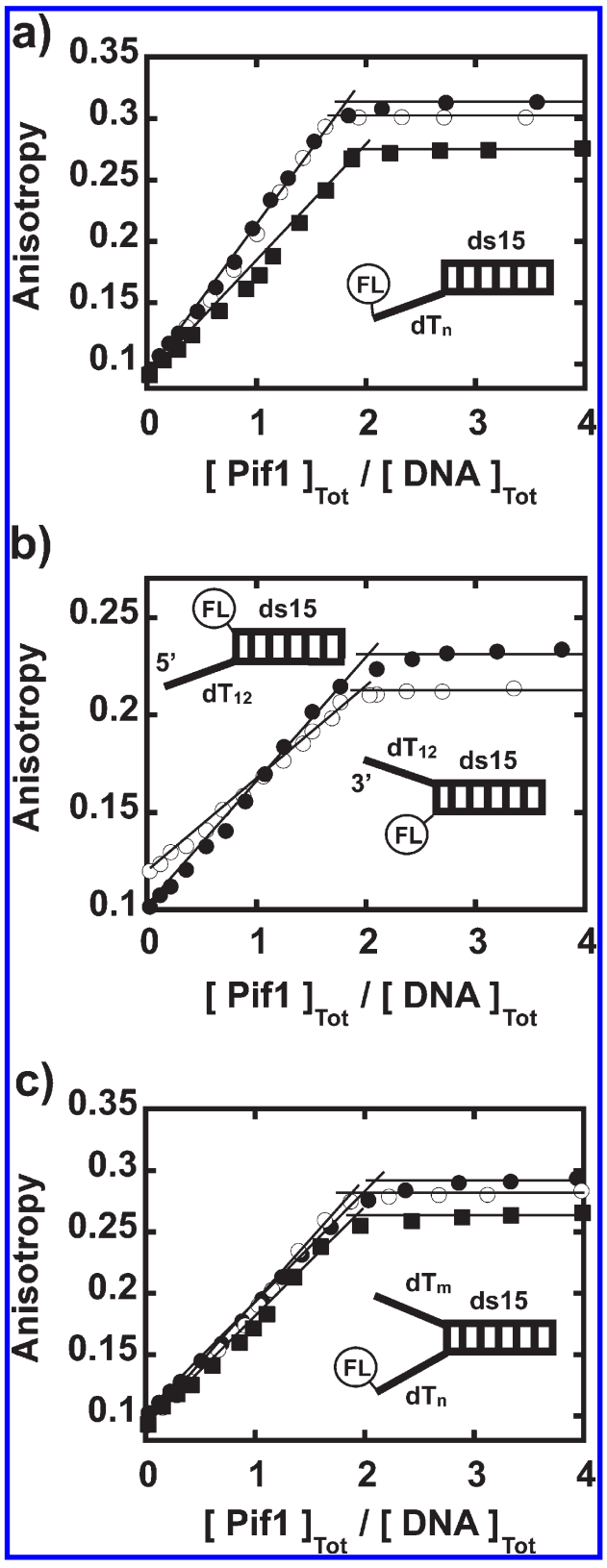


FIGURE 5: DNA-induced dimerization of Pif1 on tail- and fork-dsDNA substrates. (a) Stoichiometric titrations in buffer N100M-10 °C of the indicated substrate at 320 nM for $n = 5$ (●) and 250 nM for $n = 8$ (○) and $n = 10$ (■). (b) Stoichiometric titrations in buffer N100M-10 °C of the indicated substrates at 320 nM. (c) Stoichiometric titrations in buffer N100M-10 °C of the indicated substrate at 320 nM for $n = 5$ and $m = 5$ (●) and 250 nM for $n = 10$ and $m = 10$ (○), and $n = 12$ and $m = 12$ (■).

Pif1 is a 5′ to 3′ helicase (*2*, *12*, *16*), and the substrates utilized in Figure 5a have a 5′-ssDNA that can serve as a loading site for DNA

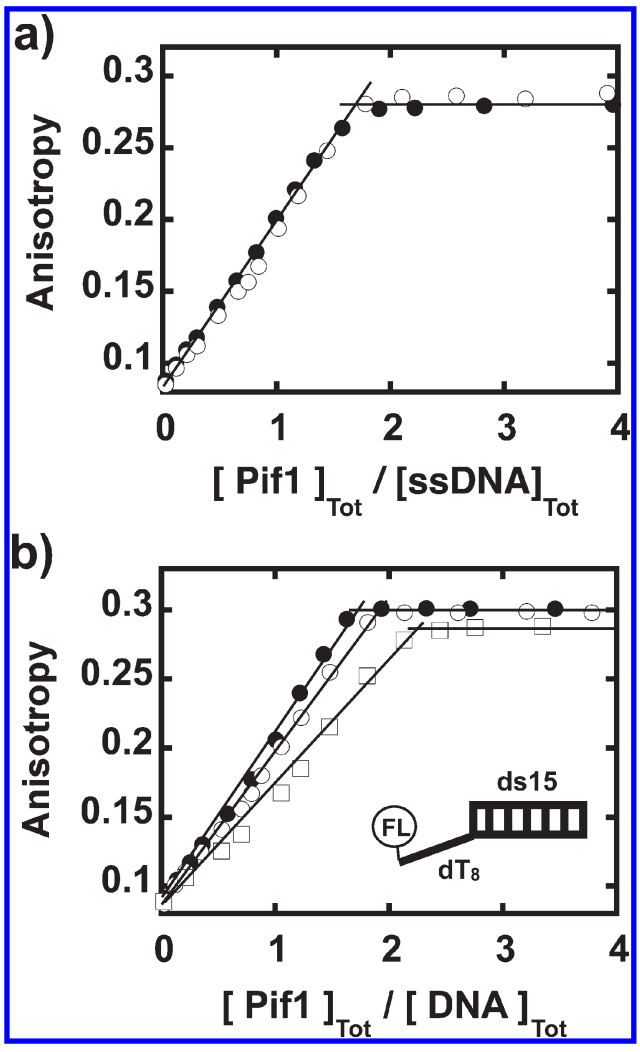


FIGURE 6: DNA-induced dimerization of Pif1 is independent of sequence composition and nucleotide cofactors. (a) Stoichiometric titrations in buffer N100M-10 °C of 320 nM FL-d(TCCGCCGC) (○) and FL-dT8 (●). (b) Stoichiometric titrations in buffer N100M-10 °C of FL-$dT_8$-ds15 at 320 nM in the presence of 2 mM AMP-PNP (○) or ATP$\gamma$S (□) and at 250 nM in the absence of the ATP analogues (●).

unwinding by Pif1 (see the Supporting Information). We examined whether the dimerization of Pif1 occurs also on DNA substrates with 3′-ssDNA tails. Binding of Pif1 to these substrates would lead to a complex that is not productive for unwinding (*2*, *12*, *16*).

We designed dsDNA substrates (15 bp long) with a 3′- or 5′-ssDNA tail of 12 nucleotides and carrying a fluorescein modification at the ssDNA−dsDNA junction (Figure 5b). Titrations under stoichiometric conditions of these substrates in buffer N100M-10 °C are shown in Figure 5b. Two Pif1 molecules bind at saturation to the substrate with a 5′-ssDNA of 12 nucleotides and the fluorescein label at the junction. This behavior is consistent with that observed with dsDNA substrates with 5′-fluorescein-labeled ssDNA tails. On these substrates, the mode of Pif1 binding is not affected by the location of the fluorescent label, as observed for ssDNA (Figure 3b). Interestingly, at saturation two Pif1 molecules bind also to the substrate with a 3′-ssDNA tail [Figure 5b (○)]. However, Pif1 does not unwind these substrates (data not shown and refs *2*, *12*, and *16*).

The observation that a dimer of Pif1 forms on dsDNA substrates with either a 5′- or a 3′-ssDNA tail prompted us to examine whether multiple molecules of Pif1 can bind to fork-DNA substrates (containing both 5′- and 3′-ssDNA tails). Titrations

under stoichiometric conditions of fork-dsDNA substrates with different lengths of a 5′-fluorescein-labeled ssDNA tail and a 3′-ssDNA tail (5′FL-dT$_n$/3′-dT$_m$-ds15 with $n$ = 5 and $m$ = 5, $n$ = 10 and $m$ = 10, and $n$ = 12 and $m$ = 12) in buffer N100M-10 °C are shown in Figure 5c. Surprisingly, in the examined range of lengths of the 5′- and 3′-ssDNA tails, two Pif1 molecules bind at saturation. Thus, on these substrates formation of a Pif1 dimer prevents binding of additional Pif1 molecules to the ssDNA tails.

*Dimerization of Pif1 Is Observed on ssDNA of Random Composition and Is Not Affected by Binding of Non-hydrolyzable ATP Analogues*. Binding of Pif1 to single-stranded homodeoxynucleotides induces dimerization of the protein. However, in its normal cellular functions, Pif1 will encounter DNA sequences of mixed composition. Therefore, we tested whether the observed mode of Pif1 binding to homo-oligonucloetides is maintained on ssDNA of random composition.

Stoichiometric titrations of 5′-fluorescein-labeled d(TCCG-CCGC) and FL-dT$_8$ in buffer N100M-10 °C are shown in Figure 6a. As for the 8-mer homo-oligonucleotide, two Pif1 molecules bind to the 8-mer of random composition. The data indicate that ssDNA-induced dimerization of Pif1 is not an exclusive property of ssDNA of homogeneous composition; it occurs also on ssDNA with random composition.

The data in Figure 5 show that in the absence of nucleotide cofactors a Pif1 dimer is formed on unwinding substrates (e.g., 5′-tail-dsDNA). Next, we tested whether binding to Pif1 of non-hydrolyzable ATP analogues affects its mode of binding.

Titrations under stoichiometric conditions of a tail-dsDNA substrate with a 5′-fluorescein-labeled dT$_8$ tail (FL-dT$_8$-ds15) in the presence of 2 mM AMP-PNP or ATPγS in buffer N100M-10 °C are shown in Figure 6b. For reference, the results from titration of the same substrate in the absence of the nonhydrolyzable ATP analogues are included. We note that the titration in the presence of ATPγS is slightly shifted toward higher Pif1:DNA ratios, suggesting a possible difference in its effect on the interaction as compared to AMP-PNP. However, in the presence of ATP analogues, two Pif1 molecules still bind to this substrate at saturation, suggesting that the dimer of Pif1 represents the pre-initiation complex leading to species responsible for unwinding (see below).

*Stable Dimers of Pif1 Formed on Fork-dsDNA Are Detected via Analytical Ultracentrifugation*. We examined the stoichiometry of Pif1 on different DNA substrates using analytical ultracentrifugation. Interestingly, using either sedimentation velocity or equilibrium, we were not able to detect stable dimers formed on the short ssDNA examined (data not shown). However, the situation is different when we employ fork-dsDNA.

Sedimentation velocity experiments were performed using dsDNA substrates with 5′-fluorescein-labeled ssDNA tails and 3′-ssDNA tails of equal length (5′FL-dT$_n$/3′-dT$_m$-ds15 with $n$ = 8 and $m$ = 8, and $n$ = 10 and $m$ = 10) and a 3-fold excess of Pif1. The data were collected at 495 nm where Pif1 does not contribute to the signal. The normalized $c(s)$ distributions of sedimentation coefficients of these substrates in the presence of excess Pif1 in buffer N100M-10 °C are shown in Figure 7a (solid lines). As a reference, we determined the $c(s)$ distribution of the same substrates alone in buffer N-22 °C (composition of N100M but without glycerol) (Figure 7a, dashed lines). Also, in Figure 7a, we include the $c(s)$ distribution of sedimentation coefficients of Pif1 alone (dotted line, data from Figure 1b). It is evident that in the presence of excess Pif1 the DNA substrates migrate with a

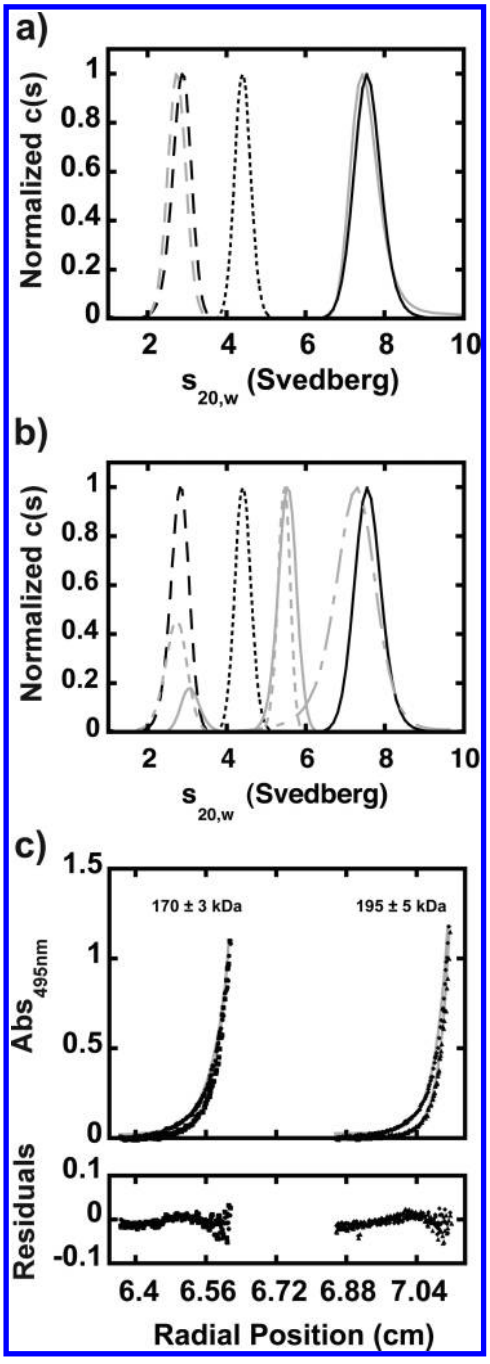


FIGURE 7: Stable Pif1 dimers are observed with both sedimentation velocity and equilibrium analytical ultracentrifugation. (a) Continuous $c(s)$ distributions as a function of $s_{20,w}$ calculated from the sedimentation velocity profiles collected in buffer N100M-10 °C at 280 nm for 8 μM Pif1 (···) and at 495 nm for 3 μM FL-dT$_8$/dT$_8$-ds15 (gray solid line) and FL-dT$_{10}$/dT$_{10}$-ds15 (black solid line) in the presence of a 3-fold excess of Pif1. The dashed lines are the $c(s)$ distributions for 3 μM FL-dT$_8$/dT$_8$-ds15 (gray) and FL-dT$_{10}$/dT$_{10}$-ds15 (black) collected at 22 °C in buffer N100M without glycerol. (b) Continuous $c(s)$ distributions of 3 μM FL-dT$_{10}$/dT$_{10}$ds15 in the presence of different Pif1:DNA loading ratios: 3:1 (black solid line), 2:1 (−-−), 1:1 (gray solid line), and 1:1.5 (gray dashed line). As a reference, the $c(s)$ distributions for free Pif1 (···) and free DNA (black dashed line) are shown as well (data from panel a). (c) Sedimentation equilibrium profiles in buffer N100M-10 °C collected at 495 nm and two different rotor speeds (15000 and 17000 rpm) of 3 μM Pif1 FL-dT$_{10}$/dT$_{10}$-ds15 (data on the left) and FL-dT$_{12}$/dT$_{12}$-ds15 (data on the right) in the presence of a 3-fold excess of Pif1. The solid gray lines are the global analyses of each set of data with a single species model (SedPhat), and the obtained $M_W$ values are given.

sedimentation coefficient that is much larger than those of the individual components. Moreover, at a Pif1:DNA ratio of 3:1, the distribution of sedimentation coefficients is symmetrical, suggesting the presence of a single homogeneous species. Although the large $s_{20,w}$ (7.4−7.5 S) suggests that the complex has a molecular weight consistent with a dimer of Pif1 on these substrates (as calculated from the *s* value with SedFit), we note that the substrates themselves have a relatively high sedimentation coefficient.

To determine whether the observed $s_{20,w}$ represents a complex of two Pif1 molecules bound to the substrates, we examined the distribution of the sedimentation coefficients obtained at different loading ratios. The $c(s)$ distributions of 5′FL-$dT_{10}$/3′-$dT_{10}$-ds15 in the presence of different Pif1 loading ratios in buffer N100M-10 °C are shown in Figure 7b. For reference, the distributions of sedimentation coefficients of free DNA substrate and Pif1 alone are included. At a Pif1:DNA loading ratio of 2:1, a large $s_{20,w}$ value is still detected; however, the distribution becomes asymmetric. At loading ratios of 1:1 and 1:1.5, we expect to populate both the complex with a single Pif1 molecule bound and free DNA (Figure 6c). Indeed, the $c(s)$ distributions show a peak with an $s_{20,w}$ value intermediate between those of the free Pif1 and the complex obtained at larger loading ratios. Moreover, at these loading ratios, we observe accumulation of free DNA substrate. These data show that the large $s_{20,w}$ value observed at saturating concentrations of Pif1 is consistent with the formation of a Pif1 dimer.

Finally, we determined the molecular weight of the complexes formed between Pif1 and fork-dsDNA substrates using sedimentation equilibrium. Sedimentation equilibrium profiles collected at 495 nm for two different rotor speeds of 5′FL-$dT_n$/3′-$dT_m$-ds15 (with $n$ = 10 and $m$ = 10, and $n$ = 12 and $m$ = 12) in the presence of a 3-fold excess of Pif1 in buffer N100M-10 °C are shown in Figure 7c. The solid lines are global analyses of the data obtained at two rotor speeds with a single species [as determined from sedimentation velocity under the same buffer conditions (Figure 7a)]. The apparent molecular weights of the complexes are 170 ± 3 and 198 ± 5 kDa for Pif1 bound to 5′FL-$dT_{10}$/3′-$dT_{10}$-ds15 and 5′FL-$dT_{12}$/3′-$dT_{12}$-ds15, respectively. These results confirm that the species with the large $s_{20,w}$ value observed in the sedimentation velocity experiments is a dimer of Pif1 formed on the DNA substrate.

## DISCUSSION

*Pif1 in Solution Is a Monomer with an Oblong Shape*. Previous work using glycerol gradient centrifugation showed that Pif1 is a monomer (*12*, *16*). We purified an active Pif1 (see the Supporting Information) without any tag (*16*) or the need of refolding procedures (*12*). Analytical equilibrium ultracentrifugation experiments are consistent with previous reports. Under the different solution conditions examined in this work, Pif1 in solution is a monomer with an $M_w$ of 91 ± 4 kDa. Sedimentation velocity analysis shows that the protein sediments in solution as a single, homogeneous species with an $s_{20,w}$ of 4.4 S. The low value of the sedimentation coefficient for a protein the size of Pif1 strongly suggests that in solution Pif1 has an oblong shape. The ratio of the frictional coefficient ($f/f_0$) is 1.64 (SedFit) (*23*−*26*), clearly larger than the unitary value expected for a sphere (*34*, *35*).

*DNA-Induced Dimerization of Pif1*. The results obtained in this work indicate that the interaction of Pif1 with DNA is more complex than previously assumed (*2*, *16*). We monitored the binding of Pif1 to fluorescently labeled DNA via the large change in the fluorescence anisotropy of the labeled substrate. Analysis under conditions of tight binding (stoichiometric) of the interaction of Pif1 with ssDNA of different lengths shows that at saturation two Pif1 molecules bind to the ssDNA. The mode of binding is independent of the location of the fluorescent probe on the ssDNA, although the detailed energetics differ (R.G. and S.B.-M., in preparation). The simplest model that can explain the observed 2:1 stoichiometry at saturating concentrations of the protein is a DNA-induced dimerization of Pif1. Indeed, analysis of the binding of Pif1 to short, labeled ssDNA (Figure 4c) shows that the observed change in fluorescence anisotropy as a function of Pif1 concentration is described well by this model.

By sequence homology, Pif1 is classified as member of the SF1-B (5′ to 3′ polarity of unwinding) family of helicases, where the *Escherichia coli* RecD helicase is the best-studied member (*3*, *16*, *36*−*38*). It has been proposed that Pif1 is the prototype member of a subfamily of helicases whose homologues can be found from yeast to humans (*3*, *37*, *38*). Interestingly, quantitative studies of two SF1 helicases from *E. coli*, UvrD and Rep (belonging to the SF1-A subgroup on the basis of their 3′ to 5′ polarity for unwinding), indicate that these helicases form dimers on DNA (*31*, *39*−*45*). The dimeric form of UvrD and Rep is proposed to be the minimal functional species responsible for unwinding *in vitro*, while monomers do not unwind dsDNA but are able to translocate on ssDNA (*39*−*44*). In this respect, our observation that, like UvrD and Rep, Pif1 dimerizes on DNA opens the possibility that regulation of the oligomeric state of Pif1 on DNA can lead to different functions of Pif1 as a dimer or monomer (see below) (*46*).

*Pif1 Dimerizes on dsDNA Substrates with a 5′- or 3′-ssDNA Tail*. In the concentration range examined, Pif1 does not interact with blunt-ended dsDNA and a 5′-ssDNA tail of at least four nucleotides is needed to form a complex with dsDNA substrates. Pif1 dimerizes on dsDNA with 5′-ssDNA tails of different lengths, suggesting that the presence of the duplex region does not affect the mode of binding. Rather, as compared to the binding of ssDNA of the same length, the presence of the duplex region stabilizes the formed Pif1 dimer (Figure 4b and R.G. and S.B.-M., in preparation). Pif1 is a 5′ to 3′ helicase, and dsDNA with 5′-ssDNA tails are substrates for unwinding by Pif1 (*2*, *12*, *16*). Under conditions of excess of Pif1 relative to the DNA utilized for unwinding experiments (Supporting Information and refs *2* and *16*), a dimer of Pif1 is bound to the substrate, suggesting that a dimeric form of Pif1 might be responsible for its helicase activity. Indeed, in the presence of nonhydrolyzable ATP analogues, the mode of Pif1 binding is unaltered (Figure 6b). Thus, the data suggest that on these substrates a dimer of Pif1 forms the pre-initiation complex (ATP bound but no hydrolysis), leading to its unwinding activity.

Interestingly, we observe DNA-induced dimerization of Pif1 also on dsDNA with a 3′-ssDNA tail. However, because of the 5′ to 3′ polarity of Pif1 helicase activity, these substrates are not unwound (data not shown) (*2*, *12*, *16*). These data suggest that although a Pif1 dimer is formed on the substrate it is not in a complex productive for unwinding, possibly due to an "inverted" orientation on the ssDNA.

*Pif1 Forms Stable Dimers on Fork-dsDNA*. The observation that Pif1 dimerizes on dsDNA with either a 5′- or 3′-ssDNA tail suggests that multiple molecules of Pif1 could bind to fork-dsDNA substrates. This is not what we observe. On fork-DNA substrates, a Pif1 dimer is formed in a manner independent of the length of the ssDNA tails, suggesting that dimerization prevents

the binding of additional Pif1 molecules. These substrates are efficiently unwound by Pif1 (*2*, *16*). Our data suggest that on fork-dsDNA Pif1 forms a dimer on the 5′-ssDNA tail and that the presence of the 3′-ssDNA tail leads to further stabilization of the complex. Studies of the unwinding reaction by Pif1 suggest that the presence of a 3′-ssDNA tail in the substrate leads to an overall increase in the efficiency of the reaction (*16*). Indeed, a stable dimer of Pif1 is detected on fork-dsDNA both with sedimentation velocity and with equilibrium analytical ultracentrifugation techniques (Figure 7). With excess Pif1 relative to fork-dsDNA (with equal lengths of the ssDNA tails), the complex sediments with an $s_{20,w}$ value larger than that expected for a single Pif1 molecule bound to this DNA. In fact, an intermediate $s_{20,w}$ value (between those of Pif1 alone and a dimer of Pif1 on the substrate) is observed at lower Pif1:DNA loading ratios, where a single molecule of Pif1 is expected to bind to the fork-dsDNA. Interestingly, using velocity and equilibrium ultracentrifugation methods we have not been able to detect stable dimers of Pif1 formed on the short ssDNA studied (5−14 nucleotides). It is possible that for these ssDNA lengths the DNA is not long enough to make contact with the second molecule of the dimer (Figure 4a), resulting in a complex that in the AUC experiments is not stable under the applied forces and relatively high viscosity of our buffer conditions. Indeed, we observe (data not shown) higher-molecular weight complexes of Pif1 with longer ssDNA (e.g., 24-mer). However, in this case, either two Pif1 molecules may bind next to each other on the lattice or both Pif1 molecules in the dimer may make contact with the ssDNA, thus leading to stabilization of a complex that can be detected with AUC experiments. The situation is different for fork-dsDNA substrates where a stable dimer of Pif1 is detected both with sedimentation velocity and with equilibrium analytical ultracentrifugation techniques. This suggests the 3′-ssDNA tail and the duplex region are sufficient to stabilize the dimer on the substrate.

*Implications of Pif1 Dimerization for Its Function*. As mentioned above, our observation that Pif1 dimerizes on DNA opens the possibility that different functional activities of Pif1 can be achieved by modulation of its oligomeric state on nucleic acid. For example, upon formation of a Pif1 dimer on DNA the complex now has two nucleotide binding sites. It is possible that binding of ATP or ADP to either or both sites leads to an allosteric regulation of DNA binding and dimerization. In the presence of saturating concentrations of nonhydrolyzable ATP analogues, a dimer of Pif1 is formed on the unwinding substrates (Figure 6b). However, allosteric modulation by ATP and ADP could lead to a different effect on the DNA binding and dimerization depending on the structure of the DNA (e.g., ssDNA vs tailed-dsDNA vs forked-dsDNA). Also, similar to other members of the SF1 class of helicases (e.g., UvrD and Rep), it is possible that regulation of the oligomeric state of Pif1 on DNA could lead to different activities (e.g., helicase vs translocase). Under conditions where a dimer is formed on unwinding substrates ([Pif1] ≫ [DNA]), Pif1 has helicase activity (refs *2* and *16* and the Supporting Information). Whether a monomer also has helicase activity remains an open question we are investigating; however, it is tempting to speculate that the functional form of Pif1 responsible for its unwinding activity is a dimer, while a monomer might be able to translocate only along ssDNA.

Finally, we show in this study that DNA-induced dimerization of Pif1 occurs on homodeoxynucleotides. A similar behavior is observed on ssDNA of random sequence (Figure 6a), although the detailed energetics are different (R.G. and S.B.-M., in preparation). However, in its function at telomeres, Pif1 will interact with the highly G-rich ssDNA at the 3′-end of the chromosome. In *S. cerevisiae*, the sequence of the 3′-ssDNA overhang of telomeres is dictated by the sequence of the template region of the telomerase RNA, leading to an irregular array of repeats, with a general consensus sequence $G_{2-3}(TG)_{1-6}$ (*47*, *48*). Whether the peculiar sequence composition or possible higher-order structures of the telomeric ssDNA affect the binding and dimerization of Pif1 and thus its role at telomeres is currently unknown.

## ACKNOWLEDGMENT

We thank T. M. Lohman, W. M. Bujalowski, and E. Di Cera for insightful and stimulating discussions.

## SUPPORTING INFORMATION AVAILABLE

Detailed methods for purification of Pif1, characterization of its basic enzymatic properties, and derivation of eq 5. This material is available free of charge via the Internet at http://pubs.acs.org.

## REFERENCES

1. Ivessa, A. S., Zhou, J. Q., Schulz, V. P., Monson, E. K., and Zakian, V. A. (2002) *Saccharomyces* Rrm3p, a 5′ to 3′ DNA helicase that promotes replication fork progression through telomeric and subtelomeric DNA. *Genes Dev. 16*, 1383–1396.
2. Boule, J. B., Vega, L. R., and Zakian, V. A. (2005) The yeast Pif1p helicase removes telomerase from telomeric DNA. *Nature 438*, 57–61.
3. Boule, J. B., and Zakian, V. A. (2006) Roles of Pif1-like helicases in the maintenance of genomic stability. *Nucleic Acids Res. 34*, 4147–4153.
4. Azam, M., Lee, J. Y., Abraham, V., Chanoux, R., Schoenly, K. A., and Johnson, F. B. (2006) Evidence that the *S. cerevisiae* Sgs1 protein facilitates recombinational repair of telomeres during senescence. *Nucleic Acids Res. 34*, 506–516.
5. Wang, X., and Baumann, P. (2008) Chromosome fusions following telomere loss are mediated by single-strand annealing. *Mol. Cell 31*, 463–473.
6. Budd, M. E., Reis, C. C., Smith, S., Myung, K., and Campbell, J. L. (2006) Evidence suggesting that Pif1 helicase functions in DNA replication with the Dna2 helicase/nuclease and DNA polymerase δ. *Mol. Cell. Biol. 26*, 2490–2500.
7. Zhou, J., Monson, E. K., Teng, S. C., Schulz, V. P., and Zakian, V. A. (2000) Pif1p helicase, a catalytic inhibitor of telomerase in yeast. *Science 289*, 771–774.
8. Lahaye, A., Stahl, H., Thines-Sempoux, D., and Foury, F. (1991) PIF1: A DNA helicase in yeast mitochondria. *EMBO J. 10*, 997–1007.
9. Schulz, V. P., and Zakian, V. A. (1994) The *Saccharomyces* PIF1 DNA helicase inhibits telomere elongation and de novo telomere formation. *Cell 76*, 145–155.
10. Doudican, N. A., Song, B., Shadel, G. S., and Doetsch, P. W. (2005) Oxidative DNA damage causes mitochondrial genomic instability in *Saccharomyces cerevisiae*. *Mol. Cell. Biol. 25*, 5196–5204.
11. O'Rourke, T. W., Doudican, N. A., Mackereth, M. D., Doetsch, P. W., and Shadel, G. S. (2002) Mitochondrial dysfunction due to oxidative mitochondrial DNA damage is reduced through cooperative actions of diverse proteins. *Mol. Cell. Biol. 22*, 4086–4093.
12. Lahaye, A., Leterme, S., and Foury, F. (1993) PIF1 DNA helicase from *Saccharomyces cerevisiae*. Biochemical characterization of the enzyme. *J. Biol. Chem. 268*, 26155–26161.
13. Ivessa, A. S., Zhou, J. Q., and Zakian, V. A. (2000) The *Saccharomyces* Pif1p DNA helicase and the highly related Rrm3p have opposite effects on replication fork progression in ribosomal DNA. *Cell 100*, 479–489.
14. Myung, K., Chen, C., and Kolodner, R. D. (2001) Multiple pathways cooperate in the suppression of genome instability in *Saccharomyces cerevisiae*. *Nature 411*, 1073–1076.

15. Pennaneach, V., Putnam, C. D., and Kolodner, R. D. (2006) Chromosome healing by de novo telomere addition in *Saccharomyces cerevisiae*. *Mol. Microbiol. 59*, 1357–1368.
16. Boule, J. B., and Zakian, V. A. (2007) The yeast Pif1p DNA helicase preferentially unwinds RNA DNA substrates. *Nucleic Acids Res. 35*, 5809–5818.
17. Kowalczykowski, S. C., Lonberg, N., Newport, J. W., and von Hippel, P. H. (1981) Interactions of bacteriophage T4-coded gene 32 protein with nucleic acids. I. Characterization of the binding interactions. *J. Mol. Biol. 145*, 75–104.
18. Cantor, C. R., Warshaw, M. M., and Shapiro, H. (1970) Oligonucleotide interactions. 3. Circular dichroism studies of the conformation of deoxyoligonucleotides. *Biopolymers 9*, 1059–1077.
19. Bloomfield, V. A., Crothers, D. M., and Tinoco, I. J. (2000) Nucleic Acids: Structure, Properties and Functions, University Science Books, Mill Valley, CA.
20. Kallansrud, G., and Ward, B. (1996) A comparison of measured and calculated single- and double-stranded oligodeoxynucleotide extinction coefficients. *Anal. Biochem. 236*, 134–138.
21. Gill, S. C., and von Hippel, P. H. (1989) Calculation of protein extinction coefficients from amino acid sequence data. *Anal. Biochem. 182*, 319–326.
22. Pace, C. N., Vajdos, F., Fee, L., Grimsley, G., and Gray, T. (1995) How to measure and predict the molar absorption coefficient of a protein. *Protein Sci. 4*, 2411–2423.
23. Schuck, P. (2003) On the analysis of protein self-association by sedimentation velocity analytical ultracentrifugation. *Anal. Biochem. 320*, 104–124.
24. Balbo, A., Brown, P. H., Braswell, E. H., Schuck, P. (2007) Measuring protein-protein interactions by equilibrium sedimentation, Current Protocols in Immunology, Chapter 18, Unit 18, Wiley, New York.
25. Schuck, P. (1998) Sedimentation analysis of noninteracting and self-associating solutes using numerical solutions to the Lamm equation. *Biophys. J. 75*, 1503–1512.
26. Dam, J., Velikovsky, C. A., Mariuzza, R. A., Urbanke, C., and Schuck, P. (2005) Sedimentation velocity analysis of heterogeneous protein-protein interactions: Lamm equation modeling and sedimentation coefficient distributions c(s). *Biophys. J. 89*, 619–634.
27. Kumaran, S., Kozlov, A. G., and Lohman, T. M. (2006) *Saccharomyces cerevisiae* replication protein A binds to single-stranded DNA in multiple salt-dependent modes. *Biochemistry 45*, 11958–11973.
28. Ralston, G. (1993) Introduction to Analytical Ultracentrifugation, Vol. 1, Beckman Intruments, Inc.
29. Eftink, M. R. (1997) Fluorescence methods for studying equilibrium macromolecule-ligand interactions. *Methods Enzymol. 278*, 221–257.
30. Bujalowski, W., and Lohman, T. M. (1991) Monomer-tetramer equilibrium of the *Escherichia coli* ssb-1 mutant single strand binding protein. *J. Biol. Chem. 266*, 1616–1626.
31. Chao, K. L., and Lohman, T. M. (1991) DNA-induced dimerization of the *Escherichia coli* Rep helicase. *J. Mol. Biol. 221*, 1165–1181.
32. Bujalowski, W., and Lohman, T. M. (1987) A general method of analysis of ligand-macromolecule equilibria using a spectroscopic signal from the ligand to monitor binding. Application to *Escherichia coli* single-strand binding protein-nucleic acid interactions. *Biochemistry 26*, 3099–3106.
33. Bujalowski, W. (2006) Thermodynamic and kinetic methods of analyses of protein-nucleic acid interactions. From simpler to more complex systems. *Chem. Rev. 106*, 556–606.
34. Cantor, C., and Schimmel, P. (1980) Biophysical Chemistry, Vol. II, W. H. Freeman and Co., New York.
35. van Holde, K. E., Johnson, W. C., and Ho, P. S. (1998) Principles of Physical Biochemistry, Prentice Hall, Upper Saddle River, NJ.
36. Berger, J. M. (2008) SnapShot: Nucleic acid helicases and translocases. *Cell 134*, No. e881.
37. Bochman, M. L., Sabouri, N., and Zakian, V. A. (2010) Unwinding the functions of the Pif1 family helicases. *DNA Repair 9*, 237–249.
38. Bessler, J. B., Torredagger, J. Z., and Zakian, V. A. (2001) The Pif1p subfamily of helicases: Region-specific DNA helicases? *Trends Cell Biol. 11*, 60–65.
39. Fischer, C. J., Maluf, N. K., and Lohman, T. M. (2004) Mechanism of ATP-dependent translocation of *E. coli* UvrD monomers along single-stranded DNA. *J. Mol. Biol. 344*, 1287–1309.
40. Maluf, N. K., Fischer, C. J., and Lohman, T. M. (2003) A dimer of *Escherichia coli* UvrD is the active form of the helicase in vitro. *J. Mol. Biol. 325*, 913–935.
41. Maluf, N. K., Ali, J. A., and Lohman, T. M. (2003) Kinetic mechanism for formation of the active, dimeric UvrD helicase-DNA complex. *J. Biol. Chem. 278*, 31930–31940.
42. Brendza, K. M., Cheng, W., Fischer, C. J., Chesnik, M. A., Niedziela-Majka, A., and Lohman, T. M. (2005) Autoinhibition of *Escherichia coli* Rep monomer helicase activity by its 2B subdomain. *Proc. Natl. Acad. Sci. U.S.A. 102*, 10076–10081.
43. Cheng, W., Hsieh, J., Brendza, K. M., and Lohman, T. M. (2001) *E. coli* Rep oligomers are required to initiate DNA unwinding in vitro. *J. Mol. Biol. 310*, 327–350.
44. Ali, J. A., Maluf, N. K., and Lohman, T. M. (1999) An oligomeric form of *E. coli* UvrD is required for optimal helicase activity. *J. Mol. Biol. 293*, 815–834.
45. Wong, I., Chao, K. L., Bujalowski, W., and Lohman, T. M. (1992) DNA-induced dimerization of the *Escherichia coli* rep helicase. Allosteric effects of single-stranded and duplex DNA. *J. Biol. Chem. 267*, 7596–7610.
46. Lohman, T. M., Tomko, E. J., and Wu, C. G. (2008) Non-hexameric DNA helicases and translocases: Mechanisms and regulation. *Nat. Rev. Mol. Cell Biol. 9*, 391–401.
47. Wang, S. S., and Zakian, V. A. (1990) Sequencing of *Saccharomyces* telomeres cloned using T4 DNA polymerase reveals two domains. *Mol. Cell. Biol. 10*, 4415–4419.
48. Shampay, J., Szostak, J. W., and Blackburn, E. H. (1984) DNA sequences of telomeres maintained in yeast. *Nature 310*, 154–157.